Dalton Transactions



PAPER

View Article Online
View Journal | View Issue



Cite this: *Dalton Trans.*, 2023, **52**, 9582

Rearrangement of a Ge(II) aryloxide to yield a new Ge(II) oxo-cluster [Ge₆(μ_3 -O)₄(μ_2 -OC₆H₂-2,4,6-Cy₃)₄] (NH₃)_{0.5}: main group aryloxides of Ge(II), Sn(II), and Pb(II) [M(OC₆H₂-2,4,6-Cy₃)₂]₂ (Cy = cyclohexyl)†

Connor P. McLoughlin, Da Derrick C. Kaseman, Db,c James C. Fettinger Da and Philip P. Power D*

The new Ge(II) cluster [Ge₆(μ_3 -O)₄(μ_2 -OC₆H₂-2,4,6-Cy₃)₄](NH₃)_{0.5} (**1**) and three divalent Group 14 aryloxide derivatives [Ge₆(OC₆H₂-2,4,6-Cy₃)₂]₂ (**2**), [Sn(OC₆H₂-2,4,6-Cy₃)₂]₂ (**3**), and [Pb(OC₆H₂-2,4,6-Cy₃)₂]₂ (**4**) of the new tricyclohexylphenyloxo ligand, [(-OC₆H₂-2,4,6-Cy₃)₂]₂ (Cy = cyclohexyl), were synthesized and characterized. Complexes **1**–**4** were obtained by reaction of the metal bissilylamides M(N(SiMe₃)₂)₂ (M = Ge, Sn, Pb) with 2,4,6-tricyclohexylphenol in hexane at room temperature. If the freshly generated reaction mixture for the synthesis of **2** is stirred in solution for 12 h at room temperature, the cluster [Ge₆(μ_3 -O)₄(μ_2 -OC₆H₂-2,4,6-Cy₃)₄](NH₃)_{0.5} (**1**), which features a rare Ge₆O₈ core that includes ammonia molecules in non-coordinating positions, is formed. Complexes **3** and **4** were also characterized *via* ¹¹⁹Sn {¹H} NMR and ²⁰⁷Pb NMR spectroscopy and feature signals at -280.3 ppm (¹¹⁹Sn{¹H}, 25 °C) and 1541.0 ppm (²⁰⁷Pb, 37 °C), respectively. The spectroscopic characterization of **3** and **4** extends known ¹¹⁹Sn parameters for dimeric Sn(II) aryloxides, but data for ²⁰⁷Pb NMR spectra for Pb(II) aryloxides are rare. We present also a rare VT-NMR study of a homoleptic 3-coordinate Pb(II) aryloxide. The crystal structures of **2**, **3**, and **4** feature interligand H···H contacts that are similar in number to those of related transition metal derivatives despite the larger size of the group 14 elements.

Received 25th March 2023, Accepted 21st June 2023 DOI: 10.1039/d3dt00906h

rsc.li/dalton

Introduction

The main group bissilylamides $M(N(SiMe_3)_2)_2$ (M = Ge, Sn, Pb)^{1,2} are frequently employed in the synthesis of low oxidation state complexes of $Ge(\pi)$, $Sn(\pi)$, and $Pb(\pi)$ complexes, several of which can act as precursors to nanomaterials.³⁻⁵ Thus, for the Ge nanomaterials, $Ge(\pi)$ alkoxide and aryloxides have been synthesized as precursors for materials that could potentially replace silicon-based nanomaterials owing to the higher electron and hole mobility⁸ and smaller band gap in germanium species in contrast to those of silicon.⁹ In com-

parison to their Sn(II) analogs, 10-19 however, low-coordinate $Ge(\Pi)$ and $Pb(\Pi)^{12,20-22}$ complexes are relatively scarce. For example, Ge(II)-oxo dimers [Ge(OR)₂]₂, monomers Ge(OR)₂, and calixarene complexes have been reported in approximately equal numbers. 6,7,11,14-16 But, there are just three homoleptic germanium complexes of formula $[Ge(OR)_2]_2$ (R = $-C_6H_3-2,6 Pr_{2}^{i}$, $-C_{6}H_{2}-2,4,6-Me_{3}$, $-C_{6}H_{3}-2,6-Me_{2}$). For lead, only one homoleptic Pb(II) aryloxide [Pb(OC₆H₃-2,6-Ph₂)]₂ has been characterized.20 Similarly, Weinert, Guzei, Rheingold, and Sita isolated a heteroleptic Pb(II) trimethylsilanolato dimer in 1997.21 Extensive compilations of 119Sn NMR parameters for Sn(II) aryloxides can be found in reviews by Wrackmeyer,²⁴ Weinert,²⁵ and Takeuchi and Takayama.²⁶ However, ²⁰⁷Pb NMR and solution-phase ⁷³Ge NMR data for two or three-coordinate Pb(II) and Ge(II) aryloxides are very scarce. 12,24-31 We report herein the synthesis and characterization of 3-coordinate, homoleptic aryloxide dimers of Ge(II), Sn(II), and Pb(II), with the tin and lead analogues characterized by heteronuclear NMR spectroscopy. Additionally, we detail the isolation and characterization of a rare Ge6O8 aryloxo cluster formed from the rearrangement of the Ge(II) aryloxo dimer.

^aDepartment of Chemistry, University of California, Davis, California 95616, USA. E-mail: pppower@ucdavis.edu

^bNuclear Magnetic Resonance Facility, University of California, One Shields Avenue, Davis, California 95616, USA

^cBiochemistry and Biotechnology Group, Los Alamos National Laboratory, Los Alamos, New Mexico 87545, USA

[†] Electronic supplementary information (ESI) available: Nuclear magnetic resonance spectroscopy data for 1–4, infrared and UV-Vis spectroscopic data for 1–4, and X-Ray crystallographic data for 1–4. CCDC 2251543–2251546. For ESI and crystallographic data in CIF or other electronic format see DOI: https://doi.org/10.1039/d3dt00906h

Results and discussion

The synthesis of the compounds in this article involves amine elimination from the divalent group 14 element amides via the reaction with 2,4,6-tricyclohexylphenol (Scheme 1). This produces, in the first instance, the simple divalent aryloxides $M(OC_6H_2-2,4,6-Cy_3)_2$ (M = Ge, Sn, and Pb), which crystallize in good yield as the dimers $[M(OC_6H_2-2,4,6-Cy_3)_2]_2$ (M = Ge, 2; Sn, 3; Pb, 4). If the solution of complex 2 is stirred overnight at room temperature in hexanes without isolation of the aryloxide, the solution darkens from pale yellow to orange. Removing the solvent under reduced pressure and washing the crude yellow solid with cold hexane four times (ca. 5 mL) until the washings become colorless, followed by recrystallization of the remaining solids from ca. 10 mL hot (ca. 100 °C) toluene, produced colorless rectangular plates of 1 (Fig. 1). Complex 1 is a Ge₆O₈ cluster composed of two 4-coordinate Ge(II) "caps" and four 3-coordinate Ge(II) atoms. This arrangement gives alternating faces composed of four Ge2O2 rings and four Ge₃O₃ rings (Fig. S19†). There are four ammonia molecules per unit cell nestled between the flanking cyclohexyl rings of

Scheme 1 Synthesis of compounds 2-4.

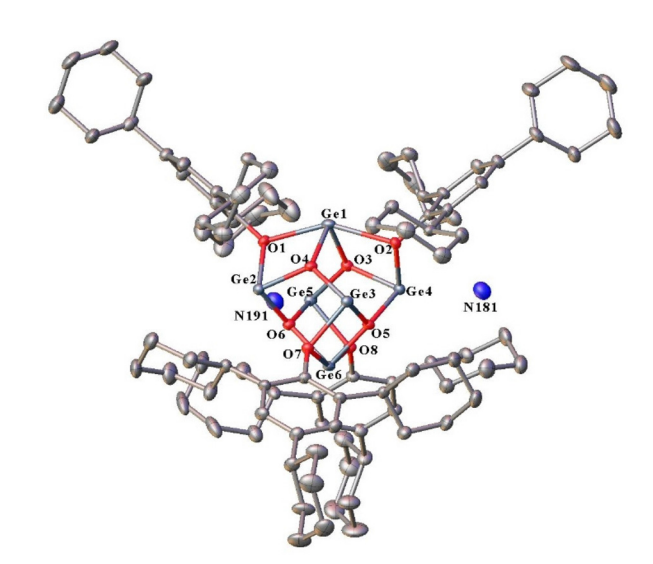


Fig. 1 Crystal structure of compound 1 featuring a Ge_6O_8 core with thermal ellipsoids shown at 30%. Co-crystallized solvent molecules (toluene) and hydrogen atoms not shown. R_1 : 0.074.

the ligand in two 25% occupancy general positions. The distance from the nitrogen atoms to the nearest $Ge(\pi)$ atom is ca. 2.86 Å. This observation is the first of its kind, as ammonia has never been reported in non-coordinating positions in $Ge(\pi)$ oxo clusters. There are extensive $H\cdots H$ contacts between the ammonia hydrogens and those of the flanking cyclohexyl rings. Placing crystals of cluster 1 under reduced pressure (ca. 0.01 torr) at ambient temperature for 30 min reveals that the ammonia molecules are tenaciously held between the cyclohexyl substituents of the aryloxo ligands, since an $\nu N-H$ absorption at 3610 cm⁻¹ is observable in the IR spectrum.

Few instances of Ge(II) dimers rearranging to form "Ge_rO₁" clusters exist in the literature. The first examples, which yielded $[Ge_4(\mu-O)_2(OC_6H_3-2-Bu^t-4-Me)_4\cdot NH_3]_2$ and $[Ge_8(\mu_3-4-Me)_4\cdot NH_3]_2$ $O_{6}(OC_{6}H_{3}-2-Bu^{t}-4-Me)_{4}$ were reported by the group of Weinert in 2009.32 Weinert and coworkers determined that the driving force for the rearrangement and subsequent generation of similar clusters is a result of the formation of a silyl ether and ammonia, produced from a side reaction between the substituted phenol and HN(SiMe₃)₂. ³² To check if cluster 1 is formed from the decomposition of 2 (Fig. 2) in solution over time or *via* a similar mechanism to that reported by Weinert, ³² pure 2 was placed in an NMR tube and monitored by ¹H NMR spectroscopy over 14 days. These showed that 2 is stable in deuterated toluene at room temperature when protected from air and moisture. The same sample was then exposed to the atmosphere under ambient conditions for 24 h and analysis via ¹H NMR spectroscopy did not indicate the formation of 1.

The synthesis of complex 1 was repeated in hexane at room temperature with a 3:4 Ge(II) to phenol ratio, since the aryloxo ligands are also the source of the μ_3 -oxo ligands in the cluster, 32 and stirred overnight in a hexane solution which produced crystalline 1. Notably, previously reported rearrangements occurred with ligands lacking substituents at one or both *ortho*-positions of the aryl ring. 32 Thus, the formation of

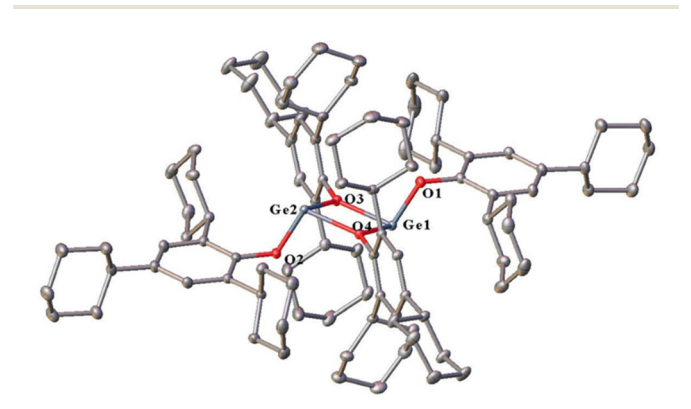


Fig. 2 Crystal structure of $[Ge(OC_6H_2-2,4,6-Cy_3)_2]_2$ (2) with thermal ellipsoids shown at 30%, hydrogen atoms are not shown. *R*1: 0.034. Selected distances (Å) and angles (°): $Ge\cdots Ge$ 3.2593(6) Å. Ge1-O1 1.8300(10) Å. Ge1-O3 2.0056(10) Å. Ge1-O4 2.0070(10) Å. Ge2-O2 1.8324(10) Å. Ge2-O3 2.0087(10) Å. Ge2-O4 2.0042(10) Å. O1-Ge1-O3 97.20(4)°. O1-Ge1-O4 99.01(4)°. O3-Ge1-O4 71.37(4)°. O2-Ge2-O3 99.43(4)°. O2-Ge2-O4 97.13(4)°. O3-Ge2-O4 71.37(4)°.

Paper Dalton Transactions

1 challenges the conclusions previously reported, which stated the formation of Ge(II) oxo clusters only occurs if one or both ortho positions of the ligand are lacking a substituent.³² Only one other Ge_6O_8 cluster, the $[Ge_6(\mu_3-O)_4(\mu_2-OC_6H_4-4-Bu^t)_4]$ species, has been reported to date. However, it was described in a Ph.D. dissertation but has not been published apart from a CCDC report. It was synthesized from the less sterically encumbering phenol HOC_6H_4 -4-Bu^t and $Ge(N(SiMe_3)_2)_2^{33}$ Notably, there are no NH₃ molecules present which render the molecular formula and structure of cluster 1 unique. The average μ_2 -O-Ge distances in complex 1 are longer than those in the closely related $[Ge_6(\mu_3-O)_4(\mu_2-OC_6H_4-4-Bu^t)_4]^{33}$ cluster by ca. 0.077 Å (Table 1) with a similar variation in the individual distances, while the average µ₃-O-Ge distances are shorter by ca. 0.047 Å with less variation than those observed in $[Ge_6](\mu_3$ $O_4(\mu_2-OC_6H_4-4-Bu^t)_4$]. Likewise, the average C-O distances are longer and have a smaller variation in distance than those in all of the reported clusters, which vary between 1.373 Å-1.409 Å.

Complex 2 features a dimeric arrangement of two Ge (OC₆H₂-2,4,6-Cy₃)₂ units in which two bridging and two terminal aryloxide ligands adopt a trans configuration (Fig. 3). The trans arrangement of the ligands is analogous to those in known dimeric Ge(II) aryloxides (Table 2),6,23 although such examples remain uncommon despite interest in the application of Ge(II) alkoxy and aryloxy precursors for nanomaterials. 6-8 The terminal Ge-O bond lengths of 1.831(2) Å (ave.) are slightly (ca. 0.009 Å) longer than those in [Ge $(OC_6H_3-2,6-Me_2)_2]_2^6$ (av. 1.822(21) Å), while the average bridging Ge-O distance of 2.006(3) Å is slightly longer by ca. 0.022 Å (Table 2). The Ge...Ge separation is also longer by ca.

Table 1 Selected distances and angles in 1 and in other "Ge_xO_v" clusters

Complex	μ ₂ -O–Ge (Å) (average)	μ ₃ -O-Ge (Å) (average)	C-O (Å) (average)
[Ge ₆ (μ_3 -O) ₄ (μ_2 -OC ₆ H ₂ -2,4,6-Cy ₃) ₄]	2.127(17)	1.923(3)	1.408(5)
$(NH_3)_{0.5}$ (1) $[Ge_6(\mu_3-O)_4(\mu_2-OC_6H_4-4-Bu^t)_4]^{33}$ $[Ge_4(\mu-O)_2(OC_6H_3-2-Bu^t-4-3)^{3/2}$	2.05(16) 1.784(2)	1.97(14) N/A	1.375(7) 1.384(4)
Me) ₄ ·NH ₃] ₂ 32 [Ge ₈ (μ ₃ -O) ₆ (OC ₆ H ₃ -2-Bu ^t -4-Me) ₄] ³²	N/A	1.920(26)	1.392(9)

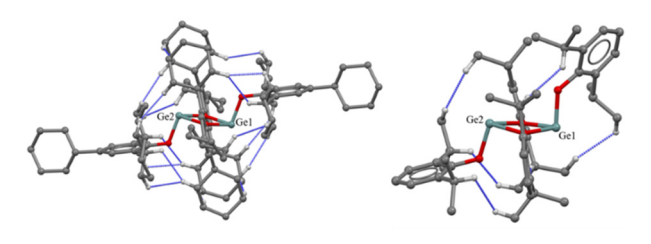


Fig. 3 Interligand H···H close (≤2.4 Å) contacts in [Ge(OC₆H₂-2,4,6-Cy₃)₂]₂ (2, left) and the sterically related complex [Ge(OC₆H₃-2,6-Prⁱ₂)₂]₂ (right).²³ Interligand H...H close contacts are shown in blue, hydrogen atoms not in close contact are not shown.

Table 2 Selected average distances (Å) and angles (°) in 2 and related [Ge(OR)₂]₂ dimers

Complex	Ge…Ge	Terminal	Bridging
	(Å)	Ge–O (Å)	μ ₂ -O–Ge (Å)
$\begin{array}{l} \left[\text{Ge}(\text{OC}_6\text{H}_22,4,6\text{-Cy}_3)_2 \right]_2(2) \\ \left[\text{Ge}(\text{OC}_6\text{H}_32,6\text{-Pr}^i_2)_2 \right]_2^{-23} \\ \left[\text{Ge}(\text{OC}_6\text{H}_22,4,6\text{-Me}_3)_2 \right]_2^{-23} \\ \left[\text{Ge}(\text{OC}_6\text{H}_32,6\text{-Me}_2)_2 \right]_2^{-6} \end{array}$	3.2593(6)	1.831(2)	2.006(2)
	3.2115(4)	1.824(1)	1.997(15)
	3.2090(8)	1.825(4)	1.984(2)
	3.1991(12)	1.822(21)	1.984(7)

0.06 Å, likely as a result of the increase in steric pressure on changing from methyl to cyclohexyl substituents. Similarly, the Ge···Ge distance, terminal Ge-O and bridging μ₂-O-Ge distances are all longer (Table 2) in $[Ge(OC_6H_2-2,4,6-Cy_3)_2]_2$ (2) than in [Ge(OC₆H₂-2,4,6-Me₃)₂]₂.²³ A comparison of bond lengths in complex 2 to those in $[Ge(OC_6H_3-2,6-Pr_2^i)_2]_2^{23}$ is consistent with the steric similarity of isopropyl and cyclohexyl substituents. 34,35 The Ge...Ge distance in 2 is ca. 0.048 Å longer than in [Ge(OC₆H₃-2,6-Prⁱ₂)₂]₂ while the average terminal Ge-O distances are similar (ca. 0.007 Å). The average bridging μ_2 -O-Ge distances in 2 are slightly longer (ca. 0.009 Å), but this value is misleading as one of the four μ_2 -O-Ge bond lengths in $[Ge(OC_6H_3-2,6-Pr_2^i)_2]_2$ is identical (2.008(2) Å), one is longer (2.012(2) Å), and the remaining two are shorter (1.981 (2) Å and 1.988(2) Å) than those in 2 (Fig. 2). The melting point of 2 is significantly lower (by ca. 12 °C) than those of its heavier congeners Sn and Pb, despite having a similar amount of interligand H···H close contacts between discrete molecules in the solid-state structure. Complex 2 crystallizes as colorless rectangular plates from toluene and hexane, but solutions of 2 are pale yellow in both solvents. Accordingly, the UV-Vis spectrum shows two absorbances, with one in the visible region, at 283 $(7863\varepsilon/M^{-1} \text{ cm}^{-1})$ and 338 nm $(3200\varepsilon/M^{-1} \text{ cm}^{-1})$. The ¹H NMR spectrum shows broadening of various signals in the alkyl region indicative of a dynamic system with potential exchange between terminal and bridging aryloxo ligands as well as inversion of the trans arrangement of the Ge₂O₂ rhomboid center.²³ A comparison of the number of interligand H···H close contacts ($\leq 2.4 \text{ Å}$) in $[Ge(OC_6H_3-2,6-Pr_2^i)_2]_2^{23}$ to [Ge $(OC_6H_2-2,4,6-Cy_3)_2$ (2) demonstrates that despite slight increases in bond lengths, there is a substantial increase in dispersion energy donor^{36,37} interactions in the case of 2 (Fig. 3). $[Ge(OC_6H_3-2,6-Pr_2^i)_2]_2$ features six interligand H···H close contacts, with four of the six contacts originating from a methyne hydrogen on the isopropyl substituents. In contrast, [Ge(OC₆H₂-2,4,6-Cy₃)₂]₂ (2) has sixteen interligand H···H close contacts, with three originating from a methyne hydrogen on the cyclohexyl groups.

The bonding in 3 (Fig. 4) and 4 (Fig. 5) is analogous to that in 2 since both complexes are dimers with a trans configuration of the ligands. The average terminal (2.030(8) Å) and bridging (2.186(18) Å) Sn-O bond lengths in 3 lie between values reported for monomers, 11-15,17,38 dimers, 18,19 and dinuclear tin(II) calixarenes. 16 The terminal Sn2-O2 distance is ca. 0.011 Å shorter than the terminal Sn1-O1 distance, both distances are similar to the sum of the covalent radii for a

Dalton Transactions Paper

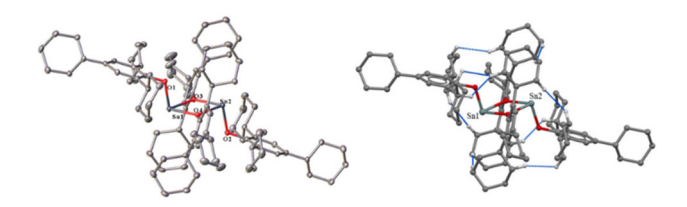


Fig. 4 Left: crystal structure of $[Sn(OC_6H_2-2,4,6-Cy_3)_2]_2$ (3) with thermal ellipsoids shown at 30%, hydrogen atoms and solvent molecules (toluene) not shown. R_1 : 0.044. Sn1-Sn2 3.5907(7) Å. Sn1-O1 2.035(4) Å. Sn1-O3 2.199(4) Å. Sn1-O4 2.166(4) Å. Sn2-O2 2.024(4) Å. Sn2-O3 2.174(3) Å. Sn2-O4 2.203(4) Å. O1-Sn1-O3 95.82(14)°. O1-Sn1-O4 95.74(14)°. O3-Sn1-O4 69.65(12)°. O2-Sn2-O3 96.44(14)°. O2-Sn2-O4 96.45(14)°. O3-Sn2-O4 69.42(13)°. Right: molecular model of 3 showing interligand H···H close contacts (<2.4 Å) in blue, hydrogen atoms participating in close contacts are shown.

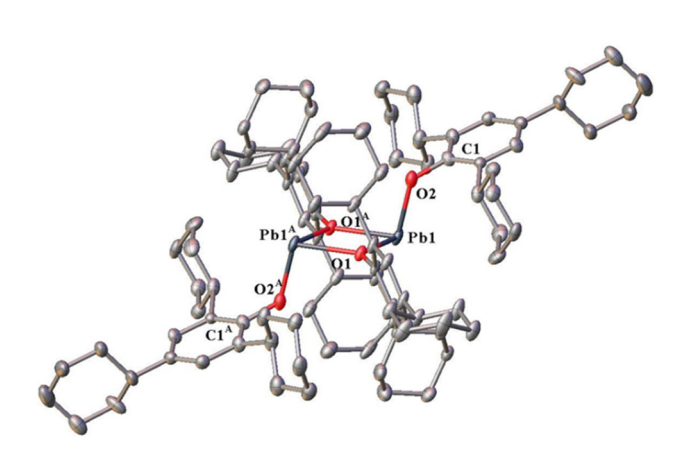


Fig. 5 Crystal structure of dimeric $[Pb(OC_6H_2-2,4,6-Cy_3)_2]_2$ (4) with thermal ellipsoids shown at 30%, with hydrogen atoms and co-crystallized solvent molecules (toluene) not shown. R1: 0.047. Selected distances (Å) and angles (°): Pb1-Pb1A 3.7725(7). Pb1-O2 2.117(6). Pb1-O1 2.284(4). Pb1-O1A 2.302(4). O1-Pb1-O2 93.87(17). O2-Pb1-O1A 98.65 (17). O1-Pb1-O1A 69.34(15).

Sn-O single bond (2.03 Å).³⁹ A similar characteristic is observed in the bridging bonds of complex 3 as the Sn1-O4 and Sn2-O3 distances are shorter than the Sn1-O3 and Sn2-O4 distances by ca. 0.03 Å, resulting in the larger standard deviation in the average Sn-O distances for both the terminal and bridging Sn-O bonds. There are nine interligand H···H contacts in $[Sn(OC_6H_2-2,4,6-Cy_3)_2]_2$ (3) while there are sixteen in $[Ge(OC_6H_2-2,4,6-Cy_3)_2]_2$ (2). The decrease in the number of H···H close contacts is likely due to the increase in M-O (M = Ge, Sn) bond distances, since the radii of Ge and Sn differ by 0.19 Å.³⁹ Multiple heteroleptic Sn(II) aryloxo dimers ligated by similar ligands to 2,4,6-tricyclohexylphenol have been

reported, 10,18,19 with the majority of the homoleptic examples existing as monomers^{10,11,18} which are stabilized by bulkier terphenyl or calixarene ligands. 12-16,38 Reactions of the sterically unencumbering phenol HOC₆H₄-2-Me with [Sn(NMe₂)₂]₂ produced a polymeric structure $[Sn(\mu-OC_6H_4-2-Me)_2]_{\infty}$, while HOC₆H₃-2,6-Me₂ and HOC₆H₃-2,6-Prⁱ₂ formed dimers, with the latter ligated by one NMe2 group at one of the Sn(II) centers. 18 In contrast, the reaction of HOC₆H₃-2,6-Bu^t₂ with [Sn(NMe₂)₂]₂ afforded a monomer, ¹⁸ which is similar in structure to Lappert and Atwood's M(OAr)₂ monomers {M = Ge, Sn, Pb, Ar = $-C_6H_2-2,4,6-Bu_3^t$ or $-C_6H_2-2,6-Bu_2^t-4-Me$.¹¹

Available data for both monomeric 22,22,28 and dimeric 20,21 homoleptic Pb(II) aryloxides are limited, with the former representing the majority by a substantial (6:1) margin. A comparison of reported Pb-O bond lengths to those of 4 (Fig. 5) shows that the terminal Pb-O bonds (av. 2.128(2) Å) in 4 are shorter than those in $Pb(OC_6H_3-2,6-(C_6H_3-2,6-Pr_2^{i_2})_2)^{2}$ presumably as a result of the steric requirements of the terphenyl in comparison to those of the 2,4,6-tricyclohexylphenoxo ligand. The bond lengths in 4 are also similar to those in the monomeric and 4-coordinate Pb(II) calixarenes [Pb(thiacalix[4] arene^{t-Bu}(O)₂(OSiⁱPr₃)₂] and [Pb(thiacalix[4]arene^{t-Bu}(O)₂(OBn)₂] (Bn = benzyl), respectively. 12 The terminal (2.117(6) Å) and bridging (2.293(10) Å) Pb-O bonds in 4 are shorter than those in the dimer [Pb(OC₆H₃-2,6-Ph₂)]₂.²⁰ Both terminal and bridging C-O distances in [Pb(OC₆H₃-2,6-Ph₂)]₂ are shorter than those of complex 4 by ca. 0.11 Å and ca. 0.018 Å, respectively, despite the increase in size of the aryl ring substituents. However, the terminal and bridging Pb-O distances in [Pb $(OC_6H_3-2,6-Ph_2)$ ₂ are significantly longer than those in 4 by ca. 0.13 Å and ca. 0.054 Å, respectively, while the Pb···Pb separation is also longer by ca. 0.061 Å (Table 3). There are eight interligand H···H close ($\leq 2.4 \text{ Å}$) contacts in [Pb(OC₆H₂-2,4,6- Cy_3 ₂₂ (4), while there is only one present in [Pb(OC₆H₃-2,6-Ph₂)]₂ (Fig. 6). Due to the greater inductive effect of the phenyl residue compared to cyclohexyl, in addition to the π -donating capability of the phenyl group, the expected Pb-O and Pb···Pb distances should be shorter in [Pb(OC₆H₃-2,6-Ph₂)]₂ than in 4 as a result of greater electrostatic interaction. However, we observe shorter distances in 4, and we propose that the increase in dispersion energy donor interactions upon exchanging the ortho substituents of [Pb(OC₆H₃-2,6-Ph₂)]₂ for the cyclohexyl groups in [Pb(OC₆H₂-2,4,6-Cy₃)₂]₂ is responsible for the decrease in Pb-O and Pb···Pb distances, counter to the steric considerations. Notably, the $[Pb(OC_6H_3-2,6-Ph_2)]_2^{20}$ complex is the only other 3-coordinate Pb(II) aryloxide dimer included in the Cambridge Crystallographic Structural Database.

Analysis of 3 via 119 Sn 1H NMR spectroscopy confirms that the structure remains associated in solution at room tempera-

Table 3 Comparison of selected average bond lengths (Å) in $[Pb(OC_6H_2-2,4,6-Cy_3)_2]_2$ (4) and $[Pb(OC_6H_3-2,6-Ph_2)]_2^{20}$

Complex	Pb···Pb	Terminal Pb-O	Bridging Pb-O	Terminal C-O	Bridging C-O
$\frac{\left[\text{Pb(OC}_{6}\text{H}_{2}\text{-}2,4,6\text{-Cy}_{3}\right)_{2}\right]_{2}}{\left[\text{Pb(OC}_{6}\text{H}_{3}\text{-}2,6\text{-Ph}_{2})\right]_{2}^{20}}$	3.7725(7)	2.117(6)	2.293(10)	1.458(9)	1.387(7)
	3.833(8)	2.243(20)	2.347(26)	1.352(13)	1.369(9)

Paper Dalton Transactions

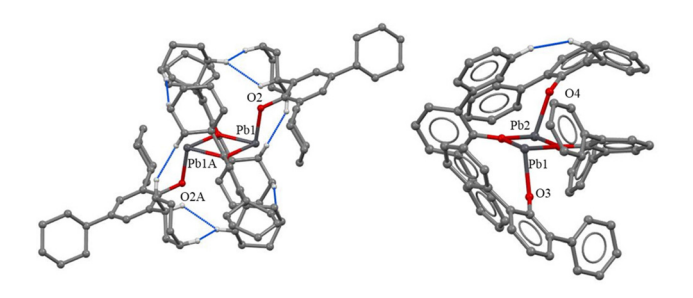


Fig. 6 Interligand H···H close (\leq 2.4 Å) contacts in [Pb(OC₆H₂-2,4,6-Cy₃)₂]₂ (4, left) and [Pb(OC₆H₃-2,6-Ph₂)]₂ (right).²⁰ Interligand H···H close contacts are shown in blue, hydrogen atoms not in close contact are not shown.

ture. Only one 119 Sn signal is observed at -280 ppm. From literature values, 10,12,24 the expected shift of 3 should fall in the narrow range of +138 to -350 ppm observed for dimeric, 3-coordinate Sn(II) alkoxides and aryloxides (Table 4). A higher temperature was not required to observe the 119 Sn NMR resonance as the solubility of 3 in deuterated toluene was sufficient to observe a signal at room temperature. Due to the temperature sensitive nature of 119 Sn NMR chemical shifts, the sample was not subjected to variable temperature 119 Sn 1 H 1 NMR studies. 10,24

Few ²⁰⁷Pb NMR data are available for Pb(II) aryloxides, ^{12,22,27,28,30,31} and data for 3-coordinate Pb(II) aryloxide dimers were nonexistent. The majority of reported ²⁰⁷Pb NMR chemical shifts concern lead compounds of biological relevance, ²⁹ such as the calmodulin-type molecules which are bound to lead for toxicological studies. Coordination complexes of Pb(II) bound to EDTA have been heavily investigated. ²⁸ While several complexes with structures similar to 4 have been reported (*vide supra*), no ²⁰⁷Pb NMR parameters were given. Therefore, we estimated the shift of complex 4 (*vide infra*) based on data for 2-coordinate aryloxides of Pb(II) (Table 5). For 2-coordinate examples, the most relevant struc-

Table 4 119 Sn NMR chemical shifts for two and three coordinate Sn(II) alkoxides and aryloxides 25 $^{\circ}$ C unless otherwise indicated. A comprehensive list of 119 Sn NMR parameters for compounds with Sn-chalcogen bonds can be found in a ref. 24

Compound ^a	δ ¹¹⁹ Sn NMR (ppm)
$\begin{split} & \sum_{\substack{[Sn(\text{thiacalix}[4]\text{arene}^{f\text{-Bu}}(O)_2(\text{OBn})_2]^{12} \\ [Sn(\text{thiacalix}[4]\text{arene}^{f\text{-Bu}}(O)_2(\text{OSi}^1\text{Pr}_3)_2]^{12}} \\ [Sn(\mu\text{-OSiPh}_3)(\text{OSiPh}_3)]_2^{10}} \\ [[DMP)\text{Sn}(\mu\text{-DMP})]_2^{10} \\ [[DMP)\text{Sn}(\mu\text{-DMP})]_2^{13} \\ [Sn(\mu\text{-OC}_6H_2\text{-}2,4,6\text{-Cy}_3)(\text{OC}_6H_2\text{-}2,4,6\text{-Cy}_3)_2} \\ [Sn(\mu\text{-OiPr})(\text{OSiPh}_3)]_2^{10} \\ [Sn(\mu\text{-OSiPh}_3)(\text{Cl})]_2^{10}} \\ [Sn(\mu\text{-OSiPh}_3)(\text{Cl})]_2^{10} \\ [Sn(\mu\text{-OPr}^1)(\text{OPr}^1)]_1^{10} \end{split}$	-647.3 -358.8 -338 -293.5 -289.7 -280.3 -246 -202 -200 (60 °C)
$[Sn(\mu-O^{1}Pr)(Cl)]_{2}^{10}$ $[Sn(OSiPh_{3})(NMe_{2})]_{2}^{10}$	-87 -38

^a DMP = dimethylpyridine; Ar^{Dipp} = $-C_6H_3$ -2,6- $(C_6H_3$ -2,6-Prⁱ₂)₂; Bn = benzyl.

Table 5 Selected ^{207}Pb NMR parameters for Pb(II) aryloxides related species

Compound ^a	δ^{207} Pb NMR (ppm)
[Pb(EDTA)] ²⁻ (ref. 28)	2441
$Pb(EDTA-N_2)^{28}$	2189
$[Pb(OC_6H_2-Cy_3)_2]_2$ (4)	1541.0 (37 °C)
[Pb(thiacalix[4]arene ^{t-Bu} (O) ₂ (OSi ^t Pr ₃) ₂] ¹²	1210
$ \begin{array}{l} [Pb(OC_6H_2\text{-}Cy_3)_2]_2 \ (4) \\ [Pb(thiacalix[4]arene^{t\text{-}Bu}(O)_2(OSi^iPr_3)_2]^{12} \\ Pb(OAr^{Dipp})_2 \ ^{22} \end{array} $	1070.3
Pb(OAr ^N) ₂ 30	141.5
[Pb(thiacalix[4]arene ^{t-Bu} (O) ₂ (OBn) ₂] ¹²	111
PbL ³¹	-367

 a L = (R,R)-(_)-N,N'-bis(3,5-di-tert-butylsalicylidene)-1,2-cyclo-hexanediamine; OAr $^{\rm Dipp}$ = OC $_6$ H $_3$ -2,6- $(C_6$ H $_3$ -2,6-Pr $^{\rm i}_2)_2$; OAr $^{\rm N}$ = 2,4-di-tert-butyl-6-(1,4,7-trioxa-10-azacyclododec-10-ylmethyl)phenyl; Bn = Benzyl.

ture is $Pb(OC_6H_3-2,6-(C_6H_3-2,6-Pr_2^i)_2)$, which featured a ^{207}Pb NMR resonance at +1070 ppm. ²² Several 4-coordinate Pb(II) calixarenes featured resonances in the range +111 ppm to +1210 ppm. ¹²

As in the ¹¹⁹Sn NMR spectroscopic studies, the ²⁰⁷Pb NMR chemical shifts depend heavily upon coordination number, temperature, and electronegativity of the ligating atoms. ²⁷ Given that complex 4 has 3-coordinate Pb(II) atoms, we expected to observe the signal between +1210 ppm and +100 ppm. However, the resonance was located further upfield than that of the two-coordinate complex Pb(OC₆H₃-2,6-(C₆H₃-2,6-Prⁱ₂)₂) at +1541 ppm. It should be noted that the signal for 4 was only observable above 37 °C. Complex 4 is thermochromic, displaying a yellow color at room temperature and an orange-red color above 100 °C in both the solid state and in solution. The yellow color reappears upon returning to room

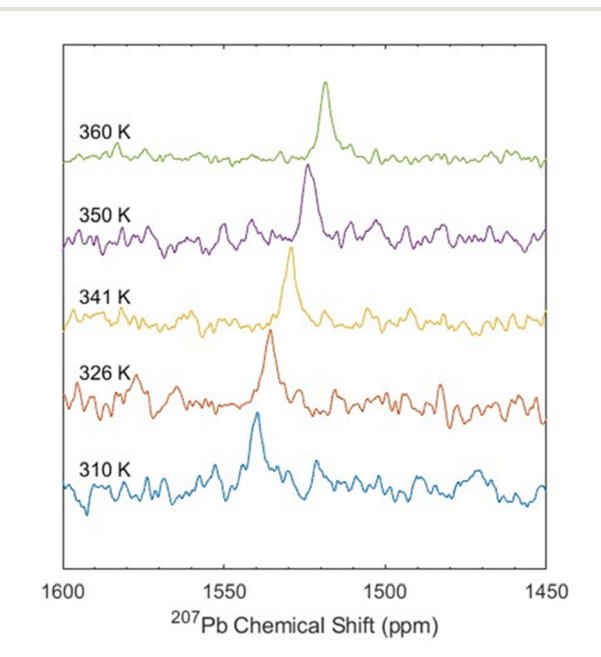


Fig. 7 207 Pb Chemical shift (ppm) as a function of temperature. 207 Pb (500 MHz, C_7D_8) (310 K) 1541 ppm, (326 K) 1534 ppm, (341 K) 1529 ppm, (350 K) 1524 ppm, (360 K) 1519 ppm.

temperature. A 207 Pb VT-NMR study was carried out due to its thermochromism and difficulty in locating the signal at room temperature. We observed the signal first at +1541 ppm, which shifts further upfield in increments of approximately 6 ppm per 10 °C of temperature change (Fig. 7) as the temperature increases. Variable temperature UV-Vis studies were carried out in toluene to observe any absorption shifts or new absorptions that appeared over the temperature to range of 25 °C to 100 °C. However, no significant changes were observed aside from a decrease in the overall absorption at each data point (Fig. S17†). The observed thermochromism in compound 4 is similar to known Pb(II) aryloxo complexes, although few are known.

Conclusions

Three divalent group 14 aryloxide complexes were synthesized via protonolysis of the metal bissilylamides with 2,4,6-tricyclohexylphenol. The complexes were characterized by X-ray crystallography, $^{119}\text{Sn}\{^1\text{H}\}$ NMR, and ^{207}Pb NMR spectroscopy. A unique cluster was isolated by stirring a solution of the germanium derivative 2 in the presence of the byproduct of its formation, namely HN(SiMe₃)₂, for 24 h in hexanes. The new complex 1 is a rare Ge_6O_8 aryloxo cluster which is the only example of a Ge_xO_y cluster formed via rearrangement of a dimeric, 3-coordinate $\text{Ge}(\Pi)$ aryloxide featuring alkyl substituents in both ortho positions of the ligand aryl rings.

Experimental section

General considerations

All manipulations were carried out under anaerobic and anhydrous conditions by using standard Schlenk techniques or in a Vacuum Atmospheres OMNI-Lab drybox under an atmosphere of dry argon or nitrogen. Solvents were dried by the method of Grubbs and co-workers, 40 stored over potassium or sodium, and then degassed by the freeze-pump-thaw method. All physical measurements were made under strictly anaerobic and anhydrous conditions. Melting points of samples in flame-sealed capillaries were determined using a Meltemp II apparatus equipped with a partial immersion thermometer. IR spectra were recorded as Nujol mulls between CsI plates on a PerkinElmer 1430 spectrometer. UV-vis spectra were recorded as dilute toluene solutions in 3.5 mL quartz cuvettes using an Olis 17 modernized Cary 14 UV-Vis-near-IR spectrophotometer. Unless otherwise stated, all materials were obtained from commercial sources and used as received. The phenol 2,4,6-tricyclohexylphenol was donated to us by Toray Industries, Inc. The main group silylamides M(N(SiMe₃)₂)₂ (M = Ge, Sn, Pb) were synthesized by published procedures. 1,2

Synthesis

 $[Ge_6(\mu_3\text{-O})_4(\mu_2\text{-OC}_6H_2\text{--}2,4,6\text{-Cy}_3)_4](NH_3)_{0.5} \ (1). \ \text{To a 100 mL}$ Schlenk flask were added 0.541 g (1.375 mmol) of Ge

(N(SiMe₃)₂)₂ and 0.6242 g (1.833 mmol) of 2,4,6-tricyclohexylphenol at room temperature in ca. 70 mL of hexanes. The yellow solution was stirred for a further 24 h without separation of the reaction byproducts (HN(SiMe₃)₂). The solvent was then removed under reduced pressure to leave a light-yellow residue which was washed with four ca. 5 mL portions of hexanes until the remaining solid had become colorless. The colorless solid was dissolved in ca. 10 mL of hot toluene and cooling in a ca. 5 °C refrigerator for 48 h produced microcrystalline material. The mother liquor was transferred to a separate flask via filter cannula and the microcrystalline solids were redissolved in ca. 3 mL of hot (ca. 100 °C) toluene. Upon cooling in a ca. 5 °C fridge for 48 h colorless rectangular blocks of 1 were collected to yield 0.0893 g (20.88%, calc. from Ge), mp 156–158 °C. ¹H-NMR (400 MHz, C₆D₆, 25 °C) 7.19 (2H), 7.14 (1H), 7.09 (1H), 7.07 (1H), 7.05 (2H), 7.03 (1H), 3.57 (1H), 3.17–2.80 (7H), 2.56 (4H), 2.05–1.26 (120H). UV-vis λ /nm $(\varepsilon/\text{M}^{-1} \text{ cm}^{-1})$ 283 (10 300). IR (Nujol; $\tilde{\nu}/\text{cm}^{-1}$) 3610 m (ν N-H), 2950s, 2910s, 2840s, 1600w, 1490w, 1450s, 1370m, 1360m, 1265w, 1255s, 1230w, 1185m, 1165m, 1090s, 1010s, 945w, 890w, 950m, 930w, 800s, 720w, 690w, 650w, 550w, 455w, 380w, 310w.

 $[Ge(OC_6H_2-2,4,6-Cy_3)_2]_2$ (2). To a 100 mL Schlenk flask were added 0.578 g (1.468 mmol) of $Ge(N(SiMe_3)_2)_2$ and 1.001 g (2.940 mmol) of 2,4,6-tricyclohexylphenol at room temperature. Hexanes (ca. 70 mL) were added via cannula and the reaction was stirred for 30 minutes. The solvent was removed under reduced pressure to leave a light-yellow residue. The flask was heated to ca. 40 °C for 30 minutes to remove the remaining volatile material under reduced pressure. The solid residue was dissolved in ca. 20 mL of hot hexane (temp. ca. 55 °C) and left to stand at room temperature. Colorless crystals of 2 precipitated from the room temperature solution after 12 h to yield 0.712 g (56.26%). Mp 238–239 °C. ¹H-NMR (400 MHz, C₇D₈, 25 °C) 7.13-7.07 (8H), 3.49 (1H), 3.10 (6H), 2.52 (4H), 1.97–1.23 (120H). UV-vis λ/nm ($\varepsilon/\text{M}^{-1}$ cm⁻¹) 283 (7863), 338 (3200). IR (Nujol; $\tilde{\nu}/\text{cm}^{-1}$) 2970s, 2940s, 2870s, 1460s, 1380s, 1360m, 1350m, 1265s, 1230w, 1190m, 1170m, 1090s, 1020s, 950w, 890w, 865w, 850w, 800s, 770w, 720w, 635w, 600w, 550w, 520w, 490w, 450w, 380w, 360w, 330w, 305w, 295w, 280w.

[Sn(OC₆H₂-2,4,6-Cy₃)₂]₂ (3). Complex 3 was prepared in a similar manner to 2 from 0.654 g (1.488 mmol) of Sn (N(SiMe₃)₂)₂ and 1.014 g (2.976 mmol) of 2,4,6-tricyclohexylphenol at room temperature. Colorless crystals of 3 precipitated from a *ca.* 30 mL toluene extract standing at room temperature for 12 h. Yield 0.587 g (49.45%). Mp > 250 °C. ¹H-NMR (400 MHz, C₇D₈, 25 °C) 7.11 (2H), 7.08–7.06 (2H), 6.96 (4H), 4.23 (1H), 4.09 (1H), 3.84 (1H), 3.40 (1H), 2.69 (4H), 2.47 (4H), 1.96–1.20 (120H). ¹¹⁹Sn{¹H} NMR (400 MHz, C₆D₆) –280.3 ppm. UV-vis λ /nm (ε /M⁻¹ cm⁻¹) 283 (7970). IR (Nujol; $\bar{\nu}$ /cm⁻¹) 2960s, 2920s, 2850s, 1460s, 1445s, 1375s, 1360m, 1350m, 1300m, 1290m, 1270m, 1260s, 1230s, 1185s, 1140s, 1105s, 1190s, 1015s, 950w, 890w, 865m, 845m, 810s, 800s, 775m, 765m, 720w, 640w, 630w, 600w, 520w, 500w, 490w, 450w, 380w, 355w, 330w.

Paper Dalton Transactions

 $[Pb(OC_6H_2-2,4,6-Cy_3)_2]_2$ (4). Complex 4 was prepared in a similar manner to 2 and 3 from 0.880 g (1.667 mmol) of Pb (N(SiMe₃)₂)₂ and 1.135 g (3.333 mmol) of 2,4,6-tricyclohexylphenol. Yellow crystals of 4 precipitated from a room temperature toluene extract (ca. 30 mL) after 3 h to yield 0.825 g (55.86%) of 4. Mp > 250 °C. ¹H-NMR $(400 \text{ MHz}, C_7D_8, 25 °C)$ 7.13 (4H), 7.08 (2H), 6.97 (2H), 3.36 (1H), 2.69 (2H), 2.56 (4H), 2.12 (5H), 1.99-1.22 (120H). ²⁰⁷Pb NMR (104.61 MHz, C₇D₈) (37 °C) 1541 ppm, (53 °C) 1534 ppm, (68 °C) 1529 ppm, (77 °C) 1524 ppm, (87 °C) 1519 ppm. UV-vis λ/nm ($\varepsilon/\text{M}^{-1}$ cm⁻¹, 25 °C) 283 (15 511), 392 (2559). IR (Nujol; $\tilde{\nu}/\text{cm}^{-1}$) 2980s, 2920s, 2850s, 2660m, 1600w, 1565w, 1490w, 1450s, 1375s, 1300s, 1290m, 1270s, 1260s, 1230s, 1190s, 1140s, 1110s, 1020s, 945w, 890w, 860s, 845m, 810s, 800s, 885m, 875m, 870m, 725m, 690w, 640w, 630w, 600w, 585w, 510w, 490w, 460w, 440w, 370w, 350w, 320w.

X-ray crystallographic studies

Crystals of 2, 3, and 4 suitable for X-ray crystallographic studies were obtained from saturated toluene solutions upon standing for 24 h. Crystals of 1 were collected from a saturated toluene solution after 48 h at 5 °C. The crystals were removed from the Schlenk tubes and immediately covered with a layer of hydrocarbon oil. Suitable crystals were selected, mounted on a nylon cryoloop, and then placed in the cold nitrogen stream of the diffractometer. Data for 2, 3, and 4 were collected at 90(2) K with Mo K α_1 radiation ($\lambda = 0.71073$ Å) using a Bruker D8 Venture dual source diffractometer in conjunction with a CCD detector while data for 1 was collected at 190(2) K with Mo $K\alpha_1$ radiation ($\lambda = 0.71073$ Å). The collected reflections were corrected for Lorentz and polarization effects and for absorption by using Blessing's method as incorporated into the program SADABS. 41,42 The structures were solved by direct methods and refined with the SHELXTL (2012, version 6.1) or SHELXTL (2013) software packages. 43 Refinement was by fullmatrix least-squares procedures, with all carbon-bound hydrogen atoms included in calculated positions and treated as riding atoms. The thermal ellipsoid plots were drawn using OLEX2 software.44

Spectroscopic parameters

¹H NMR spectra were collected on a Bruker Avance III spectrometer operating at 399.77 MHz (9.4 T). Using a 30° tip angle (4.62 µs), 16 free induction decays (FIDs) were averaged for each experiment with a 4.1s acquisition time and a repetition time of 5.1s. Variable temperature (VT) NMR experiments were collected on a Bruker Avance Neo console operating at 300.37 MHz (7.0 T). Using a 30° tip angle (5.00 μs), 16 free induction decays (FIDs) were averaged for each experiment with a 2.8 s acquisition time and a repetition time of 3.78 s. The sample was allowed to equilibrate at the temperature for 10 minutes before data collection was begun. Temperatures were calibrated on a sample of neat methanol. All spectra were internally referenced to the residual ¹H in the deuterated solvent (toluene). 119Sn{1H} (149.07 MHz) NMR spectra were collected on a Bruker Avance III spectrometer operating at 400 MHz (9.4 T). The ¹¹⁹Sn{¹H} spectra were referenced using the IUPAC referencing recommendation⁴⁵ using the frequency ratios of the solvent residual protons and the spectra were collected using a 30° tip angle (4.152 ms) with inverse-gated decoupling (WALTZ16) applied to the ¹H spins. 24 576 FIDs were averaged with an acquisition time of 260 ms and a repetition time of 760 ms. The 207Pb (104.61 MHz) NMR spectra were collected on a Bruker Avance spectrometer operating at 500 MHz (11.7 T). ²⁰⁷Pb NMR spectra were collected using a 90° pulse (7.5 ms) with 494-2048 FIDs averaged, depending on the temperature of the sample. Each FID used a 327 ms acquisition time with a 250 ms recycle delay between successive acquisitions. The 207Pb chemical shift was referenced externally to a 1 M solution of Pb(NO₃)₂ in D₂O. For the variable temperature measurements, the sample was allowed to equilibrate at the temperature for 10 minutes before data collection began. Temperatures were calibrated on a sample of neat methanol.

Conflicts of interest

There are no conflicts of interest to declare.

Acknowledgements

We thank the U.S. National Science Foundation for funding (Grant No. CHE-2152760).

References

- 1 D. H. Harris and M. F. Lappert, J. Chem. Soc., Chem. Commun., 1974, 21, 895-896.
- 2 A. J. Veinot, D. L. Stack, J. A. C. Clyburne, J. D. Masuda, D. A. Dickie, U. Chadha and R. A. Kemp, Inorg. Synth, 2018, vol. 37, 1st edn, ch. 2, pp. 26-31.
- 3 M. S. Seifner, F. Biegger, A. Lugstein, J. Bernardi and S. Barth, Chem. Mater., 2015, 27, 6125-6130.
- Hernandez-Sanchez, T. J. Boyle, H. D. Pratt, M. A. Rodriguez, L. N. Brewer and D. R. Dunphy, Chem. Mater., 2008, 20, 6643-6656.
- 5 M. R. Buck, A. J. Biacchi, E. J. Popczun and R. E. Schaak, Chem. Mater., 2013, 25, 2163-2171.
- 6 T. J. Boyle, L. J. Tribby, L. A. M. Ottley and S. M. Han, Eur. J. Inorg. Chem., 2009, 5550-5560.
- 7 H. Gerung, T. J. Boyle, L. J. Tribby, S. D. Bunge, C. J. Brinker and S. M. Han, J. Am. Chem. Soc., 2006, 128, 5244-5250.
- 8 S. M. Sze, Physics of Semiconductor Devices, 2nd ed, John Wiley & Sons, New York, 2002.
- 9 M. Kanoun, C. Busseret, A. Poncet, A. Souifi, T. Baron and E. Gautier, Solid-State Electron., 2006, 50, 1310-1314.
- 10 L. Wang, C. E. Kefalidis, T. Roisnel, S. Sinbandhit, L. Maron, J. Carpentier and Y. Sarazin, Organometallics, 2015, 34, 2139-2150.

11 B. Cetinkaya, I. Gumrukcu, M. F. Lappert, J. L. Atwood, R. D. Rogers and M. J. Zaworotko, *J. Am. Chem. Soc.*, 1980, 102, 2088–2089.

Dalton Transactions

- 12 R. Kuriki, T. Kuwabara and Y. Ishii, *Dalton Trans.*, 2020, 49, 12234–12241.
- 13 C. Stanciu, A. F. Richards, M. Stender, M. M. Olmstead and P. P. Power, *Polyhedron*, 2006, 25, 477–483.
- 14 T. Hascall, A. L. Rheingold, I. Guzei and G. Parkin, *Chem. Commun.*, 1998, 1, 101–102.
- 15 T. Hascall, K. Pang and G. Parkin, *Tetrahedron*, 2007, **63**, 10826–10833.
- 16 B. G. McBurnett and A. H. Cowley, *Chem. Commun.*, 1999, 1, 17–18.
- 17 G. D. Smith, P. E. Fanwick and I. P. Rothwell, *Inorg. Chem.*, 1990, 29, 3221–3226.
- 18 T. J. Boyle, T. Q. Doan, L. M. Steele, C. Apblett, S. M. Hoppe, K. Hawthorne, R. M. Kalinich and W. M. Sigmund, *Dalton Trans.*, 2012, 41, 9349–9364.
- 19 H. Yasuda, J. Choi, S. Lee and T. Sakakura, *J. Organomet. Chem.*, 2002, **659**, 133–141.
- 20 W. Van Zandt, J. C. Huffman and J. L. Stewart, *Main Group Met. Chem.*, 1998, 21, 237–240.
- 21 C. S. Weinert, I. A. Guzei, A. L. Rheingold and L. R. Sita, *Organometallics*, 1998, 17, 498–500.
- 22 B. D. Rekken, T. M. Brown, M. M. Olmstead, J. C. Fettinger and P. P. Power, *Inorg. Chem.*, 2013, **52**, 3054–3062.
- 23 C. S. Weinert, A. E. Fenwick, P. E. Fanwick and I. P. Rothwell, *Dalton Trans.*, 2003, 4, 532–539.
- 24 B. Wrackmeyer, Annu. Rep. NMR Spectrosc., 1999, 38, 203-264.
- 25 C. S. Weinert, *ISRN Spectrosc.*, 2012, 1–18.
- 26 T. Takeuchi and T. Takayama, *Annu. Rep. NMR Spectrosc.*, 2005, 54, 155–200.
- 27 B. Wrackmeyer and K. Horchler, *Annu. Rep. NMR Spectrosc.*, 1989, **22**, 249–306.
- 28 E. S. Claudio, M. A. ter Horst, C. E. Forde, C. L. Stern, M. K. Zart and H. A. Godwin, *Inorg. Chem.*, 2000, 39, 1391– 1397.

- 29 L. Ronconi and P. J. Sadler, Coord. Chem. Rev., 2008, 252, 2239–2277.
- 30 D. Agustin, G. Rima, H. Gornitzka and J. Barrau, Organometallics, 2000, 19, 4276–4282.
- 31 L. Wang, S. C. Roşca, V. Poirier, S. Sinbandhit, V. Dorcet, T. Roisnel, J. F. Carpentier and Y. Sarazin, *Dalton Trans.*, 2014, 43, 4268–4286.
- 32 R. A. Green, C. Moore, A. L. Rheingold and C. S. Weinert, *Inorg. Chem.*, 2009, 48, 7510–7512.
- 33 R. A. Green, A. L. Rheingold and C. S. Weinert, CSD Communication, 2019.
- 34 M. Charton, J. Am. Chem. Soc., 1975, 97, 1552-1556.
- 35 B. Pinter, T. Fievez, F. M. Bickelhaupt, P. Geerlings and F. De Proft, *Phys. Chem. Chem. Phys.*, 2012, **14**, 9846–9854.
- 36 S. Grimme, J. Comput. Chem., 2004, 25, 1463-1473.
- 37 S. Grimme, R. Huenerbein and S. Ehrlich, *ChemPhysChem*, 2011, **12**, 1258–1261.
- 38 D. A. Dickie, I. S. MacIntosh, D. D. Ino, Q. He, O. A. Labeodan, M. C. Jennings, G. Schatte, C. J. Walsby and J. A. C. Clyburne, *Can. J. Chem.*, 2008, **86**, 20–31.
- 39 P. Pyykkö and M. Atsumi, Chem. Eur. J., 2009, 15, 186– 197.
- 40 A. B. Pangborn, M. A. Giardello, R. H. Grubbs, R. K. Rosen and F. J. Timmers, *Organometallics*, 1996, **15**, 1518–1520.
- 41 G. M. Sheldrick, *SADABS, Siemens Area Detector Absorption Correction*, Göttingen Universitat, Göttingen, Germany, 2008, p. 33.
- 42 R. H. Blessing, Acta Crystallogr., Sect. A: Found. Crystallogr., 1995, 51, 33–38.
- 43 G. M. Sheldrick, *SHELXTL, Ver. 6.1*, Bruker AXS, Madison, WI, 2002.
- 44 O. V. Dolomanov, L. J. Bourhis, R. J. Gildea, J. A. K. Howard and H. Puschmann, *J. Appl. Crystallogr.*, 2009, 42, 339–341.
- 45 R. K. Harris, E. D. Becker, S. M. Cabral de Menezes, P. Granger, R. E. Hoffman and K. W. Zilm, *Pure Appl. Chem.*, 2008, 80, 59–84.